Adsorption (2011) 17: 443–452
DOI 10.1007/s10450-010-9280-8

Pressure swing adsorption for CO_2 capture in Fischer-Tropsch fuels production from biomass

Ana M. Ribeiro · João C. Santos · Alírio E. Rodrigues

Received: 10 August 2010 / Accepted: 6 October 2010 / Published online: 19 October 2010

Abstract Environmental concerns and oil price rises and dependency promoted strong research in alternative fuel sources and vectors. Fischer-Tropsch products are considered a valid alternative to oil derivatives having the advantage of being able to share current infrastructures. As a renewable source of energy, synthesis gas obtained from biomass gasification presents itself as a sustainable alternative. However, prior to hydrocarbon conversion, the bio-syngas must be conditioned, which includes the removal of carbon dioxide for subsequent sequestration and capture. A pressure swing adsorption cycle was developed for the removal and concentration of CO_2 from the bio-syngas stream. Activated carbon was chosen as adsorbent. The simulation results showed that it was possible to produce a $(H_2 + CO)$ product with a H_2/CO stoichiometric ratio of 2.14 (suitable as feed stream for the Fischer-Tropsch reactor) and a CO_2 product with a purity of 95.18%. A CO_2 recovery of 90.3% was obtained. A power consumption of 3.36 MW was achieved, which represents a reduction of about 28% when compared to a Rectisol process with the same recovery.

Keywords PSA · Fischer-Tropsch · CO_2 capture · Biomass · Biosyngas

Abbreviations

Notation

a_p	particle specific area (m^{-1})
A	virial coefficients ($m^2\ mol^{-1}$)
B	virial coefficients ($m^4\ mol^{-2}$)
Bi_i	mass Biot number of component i, $(Bi_i = \frac{a_p k_f R_p^2}{\varepsilon_p 8 D_{p,i}})$ (–)
$C_{g,i}$	gas phase concentration of component i ($mol\ m^{-3}$)
$C_{g,T}$	total gas phase concentration ($mol\ m^{-3}$)
C_p	gas mixture molar specific heat at constant pressure ($J\ mol^{-1}\ K^{-1}$)
$\overline{C_{p,i}}$	average concentration of component i in the macropores ($mol\ m^{-3}$)
$\hat{C}_{ps}$	particle specific heat at constant pressure (per mass unit) ($J\ kg^{-1}\ K^{-1}$)
$\overline{C_{p,T}}$	average total concentration in the macropores ($mol\ m^{-3}$)
$\hat{C}_{pw}$	wall specific heat at constant pressure (per mass unit) ($J\ kg^{-1}\ K^{-1}$)
C_v	gas mixture molar specific heat at constant volume ($J\ mol^{-1}\ K^{-1}$)
$C_{v,\mathrm{ads},i}$	molar specific heat of component i in the adsorbed phase at constant volume ($J\ mol^{-1}\ K^{-1}$)
$C_{v,i}$	molar specific heat of component i at constant volume ($J\ mol^{-1}\ K^{-1}$)
d_p	adsorbent particle diameter (m)
d_{wi}	internal bed diameter (m)
D_{ax}	axial dispersion coefficient ($m^2\ s^{-1}$)
$D_{c,i}$	micropore diffusivity of component i ($m^2\ s^{-1}$)
$D_{p,i}$	macropore diffusivity of component i ($m^2\ s^{-1}$)
h_f	film heat transfer coefficient between the gas and particle ($J\ s^{-1}\ m^{-2}\ K^{-1}$)
h_w	film heat transfer coefficient between the gas and wall ($J\ s^{-1}\ m^{-2}\ K^{-1}$)
k_f	film mass transfer coefficient ($m\ s^{-1}$)
K_∞	adsorption constant at infinite temperature ($mol\ kg^{-1}\ bar^{-1}$)
K_H	Henry constant ($mol\ kg^{-1}\ bar^{-1}$)
P	pressure (Pa)

A.M. Ribeiro · J.C. Santos · A.E. Rodrigues (✉)
Laboratory of Separation and Reaction Engineering (LSRE), Department of Chemical Engineering, Faculty of Engineering, University of Porto, Rua Dr. Roberto Frias, s/n, 4200-465 Porto, Portugal
e-mail: arodrig@fe.up.pt

$\overline{q_i}$ average adsorbed phase concentration of component i (mol kg^{-1})
q_i^* adsorbed concentration of component i in equilibrium with $\overline{C_{p,i}}$ (mol kg^{-1})
r_c "microparticle" radius (m)
R_g ideal gas constant (J mol^{-1} K^{-1})
R_p adsorbent particle radius (m)
t time (s)
T_g bulk phase temperature (K)
T_p solid temperature (K)
T_w wall temperature (K)
u_0 superficial velocity (m s^{-1})
y_i gas phase molar fraction of component i (–)
z axial position (m)

Greek letters

α_w ratio of the internal surface area to the volume of the column wall (m^{-1})
$(\Delta H_{ads})_i$ heat of adsorption of component i (J mol^{-1})
ε bed porosity (–)
ε_p particle porosity (–)
λ heat axial dispersion coefficient (J s^{-1} m^{-1} K^{-1})
μ bulk gas mixture viscosity (kg m^{-1} s^{-1})
ρ bulk gas mixture density (kg m^{-3})
ρ_b bed density (kg m^{-3})
ρ_p particle density (kg m^{-3})
ρ_w wall density (kg m^{-3})

1 Introduction

Recent oil price rises, political instability of the oil suppliers countries, climate changes and desire to decrease the dependency on crude oil are, nowadays, strong driving forces to the development and use of alternative energy sources and carriers. Promising candidates are Fischer-Tropsch fuels (Boerrigter 2006; Takeshita and Yamaji 2008).

The conversion of carbon monoxide and hydrogen in oxygenated compounds and hydrocarbons, at high temperature and pressure, and in the presence of an iron-based catalyst, was observed in Germany by Franz Fischer and Hans Tropsch in 1923 (Fischer and Tropsch 1926).

Nowadays Fischer-Tropsch (FT) is used commercially by Sasol, Mossgass, PetroSA and Shell. The primary products are "green" gasoline and diesel, solvents and olefins (obtained with FT at high temperatures) and waxes (obtained with FT at low temperatures) (Takeshita and Yamaji 2008; Demirbas 2009).

FT can be used to produce hydrocarbons from any carbonaceous feedstock such as coal or natural gas, which can then be refined to liquid fuels, taking advantage of the existing infrastructure (such as transportation, storage and refueling) (Takeshita and Yamaji 2008). Some additional advantages are also pointed out to the use of FT fuels in vehicles, when comparing to conventional diesel: NO_x emissions reduction due to the higher cetane number, almost complete elimination of particulate emissions due to low sulfur and aromatic content and expected reduction in hydrocarbon and CO emissions (EPA 2002; Takeshita and Yamaji 2008).

Biomass conversion to hydrocarbons by FT (Kuester and Scottsdale 1987) has recently deserved some attention due to the strict policy targets of the European Union to diversify the source of transport fuels and for reducing CO_2 emissions (Boerrigter 2006; Demirbas 2009).

All kinds of biomass feedstock, including waste material (Batdorf 2010), can be used for liquid hydrocarbon conversion by FT, thus avoiding the competition with food production and improving waste management (Demirbas 2009; Unruh et al. 2010).

2 Fischer-Tropsch Process

Figure 1 presents a schematic representation of the biomass to FT process.

The gasification yields a product gas composed of CO, CO_2, H_2O, H_2, CH_4, other gaseous hydrocarbons, tars, inorganic constituents, and ash. The outlet composition depends on the gasifier (Demirbas 2009). Some examples of units currently used for biomass gasifications are the Lurgi circulating fluid-bed and the Foster Wheeler circulating fluid-bed (Higman and van der Burgt 2008).

Different processes may be used for syngas production from biomass gasification: non-catalytic, catalytic and steam gasification (Demirbas 2009). A mixture of steam and air or

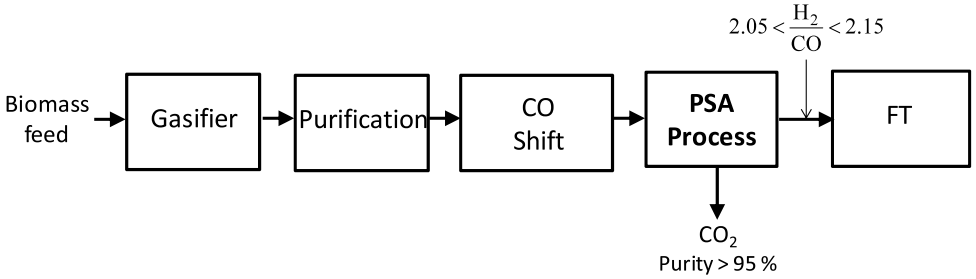

Fig. 1 Biomass to Fischer-Tropsch process

Table 1 Streams specifications

Stream		Purified syngas	After CO shift
Flow rate (kmol/h)		1500	1650
Molar fraction (%)	CO_2	20.0	27.27
	H_2	40.0	45.45
	CH_4	2.0	1.82
	CO	35.0	22.73
	N_2	3.0	2.73

oxygen is commonly used as gasifying agents in industry. The use of air reduces the heating value of the gas due to the dilution with nitrogen and increases the volume of the gas to be treated (Aasberg-Petersen et al. 2004).

The syngas has to be cleaned from impurities, such as tars, H_2S and water, (purification) and adjusted to synthesis requirements (through a CO shift step) (Unruh et al. 2010).

A typical composition of a purified syngas (that is, after the tars and H_2S removal) obtained from the gasification of biomass at 900°C with a steam to biomass weight ratio of 2.7 is presented in Table 1 (Lv et al. 2003; Yin et al. 2005). This syngas has a H_2/CO ratio of 1.1. The H_2/CO ratio at the FT reactor inlet should be in the range of 2.05 to 2.15, as required by cobalt based catalysts for promoting the formation of long chained hydrocarbons (Dry 2004; Lu and Lee 2007). A CO shift is then used to increase the H_2/CO ratio to around 2.0.

Carbon dioxide must then be captured before the Fischer-Tropsch reactor. The sequestration of CO_2 for reducing greenhouse gas emissions is an important complement of the current strategies of improving energy efficiency and increasing the use of non-fossil energy resources and should therefore be considered (Herzog 2000).

The most common technologies for CO_2 removal from syngas obtained from fossil fuels are absorbent-based systems such as the Rectisol and Selexol processes (Drage et al. 2009).

Pressure swing adsorption technology has proven to be a more economical alternative to such systems for the purification of hydrogen obtained by steam reforming. An example of such units is the Polybed process from UOP developed by Union Carbide (Fuderer and Rudelstorfer 1976). This unit, however, is unable to concentrate CO_2 for subsequent sequestration. Aware of this limitation, Air Products and Chemicals developed a PSA process called Gemini-9 comprising six parallel beds for CO_2 removal, followed by three parallel beds for H_2 purification (Kumar and Kratz 1992). This process can produce ultrapure H_2 (+99.999%) and high purity CO_2 (+99.99%) with large recoveries (>90%) for both products.

Nevertheless, the constraints of the separation required for this specific application are different from the ones required for hydrogen purification. Only CO_2 should be separated from the remaining components, for sequestration, while maintaining the H_2/CO ratio close to the inlet value (≈2). This leads to the need of developing an appropriate cycle for the PSA process. This PSA process should replace the currently used absorbent-based CO_2 removal process for syngas treatment.

3 Adsorbent and PSA cycle selection

As mentioned above, the objective of the PSA process is to separate the carbon dioxide from the feed mixture and produce it with purity above 95%, the specification required for transport and sequestration (Zhang and Webley 2008). Additionally, the H_2/CO stoichiometric ratio on the light product must be close to the H_2/CO stoichiometric ratio in the feed stream (≈2), that is, the recovery of hydrogen and carbon monoxide into the light product must be almost complete.

The hydrogen adsorptive separations processes commonly reported in the literature employ different layers of adsorbents, each with enhanced capacity for a particular impurity (silica gel or alumina for water vapor, activated carbons for carbon dioxide and methane and zeolites for carbon monoxide and nitrogen) (Chlendi and Tondeur 1995). The aim of these PSA processes is to produce 99.99+% hydrogen. However, in this case, carbon monoxide should be produced with hydrogen and only carbon dioxide should be retained to produce the heavy product. Therefore, the use of an activated carbon as a single adsorbent appears to be the best solution for this separation. Activated carbons have higher adsorption capacity towards carbon dioxide when compared to the other compounds in the feed stream. Additionally, they present weaker strength of adsorption at low pressures than zeolites which facilitates the adsorbent regeneration just by decreasing the pressure.

The activated carbon Norit R2030 was the selected adsorbent. The adsorption equilibrium and kinetics for all the compounds in the feed stream in this activated carbon have been determined by Grande et al. (2008). The Virial isotherm was used to fit the experimental adsorption data (Grande et al. 2008). The parameters obtained are given in Table 2.

The extended Virial isotherm proposed by Taqvi and LeVan (1997) for the prediction of the multicomponent adsorption equilibrium was used:

$$P_i = \frac{q_i}{K_{Hi}} \exp\left(\frac{2}{S}\sum_{j=1}^{N} A_{ij}q_j + \frac{3}{2S^2}\sum_{j=1}^{N}\sum_{k=1}^{N} B_{ijk}q_j q_k\right) \quad (1)$$

In this equation, P and q are respectively the adsorbate partial pressure and amount adsorbed, S is the adsorbent specific surface area (700 m^2/g), A and B are virial coefficients,

Table 2 Parameters of the Virial isotherm for the activated carbon Norit R2030

Compound	K_∞ [mol/(kg bar)]	$(-\Delta H)$ [J/mol]	$A_0 \times 10^{-5}$ [m^2/mol]	$A_1 \times 10^{-6}$ [m^2 K/mol]	$B_0 \times 10^{-11}$ [m^4/mol^2]	$B_1 \times 10^{-11}$ [m^4 K/mol^2]
CO_2	9.90×10^{-5}	27 870	−1.140	79.013	−0.021	−0.416
H_2	8.20×10^{-3}	3 192	0.418	−0.001	0.454	0.000
CH_4	1.04×10^{-3}	17 652	4.616	−121.43	−0.831	308.53
CO	4.62×10^{-4}	19 100	14.076	−422.77	0.264	299.25
N_2	2.54×10^{-3}	11 834	5.585	−163.77	3.385	−777.67

and K_H is the Henry constant. The Henry constant is related to the temperature (T) through the Van't Hoff equation:

$$K_H = K_\infty \exp\left(\frac{-\Delta H_{\text{ads}}}{R_g T}\right) \tag{2}$$

The mixing virial coefficients calculated by:

$$A_{ij} = \frac{(A_i + A_j)}{2} \tag{3}$$

$$B_{ijk} = \frac{(B_i + B_j + B_k)}{3} \tag{4}$$

A five step cycle was designed to accomplish this separation: adsorption, rinse, blowdown, purge and pressurization. During the adsorption step, the feed stream is fed to the column inlet and the light product (H_2 + CO) is produced on the other end. At the end of this step, the initial section of the bed (fluid and adsorbent) is in equilibrium with the feed stream. Even though the higher adsorption capacity of the activated carbon is towards carbon dioxide, it has an intermediate affinity for carbon monoxide, and therefore a fraction of the CO present in the feed stream, higher than that of H_2, will be adsorbed in the activated carbon. In order to recover this CO into the light product and also to be able to produce a 95% CO_2 product, a rinse step must be used. During the rinse step a fraction of the CO_2 product is compressed and fed to the column while the light product continues to be produced at the column outlet. After this step, the CO_2 product is obtained in the blowdown and purge steps. The blowdown decreases the column pressure countercurrently. In the purge step, a portion of the light product is fed countercurrently to the bed allowing the additional desorption of CO_2. Finally the bed is pressurized countercurrently with light product. A scheme of this cycle is presented in Fig. 2. With this design, the feed stream is separated into two product streams, without the formation of any waste.

The continuous operation of PSA processes, with constant feed consumption, involves the use of more than one bed. In this case, the cycle was extended to the 4-bed process. The corresponding extended schedule is shown in Fig. 2. This extension imposes constraints on the steps durations. Namely, the duration of the adsorption, rinse and blowdown must be the same, as well as the sum of the durations of the purge and pressurization steps. As can be seen from the extended schedule, there is, with this scheme, one column in the adsorption step at all times.

Notice should be given to the fact that the use of a pressure equalization step, commonly employed in PSA cycles to reduce the power consumption, is not advantageous in this particular case. Indeed, if a pressure equalization step was included in the cycle between the adsorption and the rinse step, the rinse step would be carried at a lower pressure and the power consumption for compressing the CO_2 would be lower. However, the outlet stream of the rinse step, which is (H_2 + CO) product, would also be at a lower pressure and would therefore require compression. Consequently the saving on power consumption on the compression of the CO_2 would be cancelled by power consumption for the compression of the (H_2 + CO) product.

4 Model

A mathematical model with mass, energy and momentum balances that represent the dynamic behavior of a non isothermal, non diluted, multicomponent adsorption bed was used to simulate the pressure swing adsorption process. The model was developed based on the following assumptions: ideal gas behavior throughout the column; no mass, heat or velocity gradients in the radial direction; constant porosity along the bed; axial dispersed plug flow; no temperature gradients inside each particle. Additionally, the model accounts for external mass and heat transfer resistances, expressed with the film model, and it considers that the adsorbent particles are bidispersed with macropore and micropore mass transfer resistances, both expressed with the Linear Driving Force (LDF) model. The momentum balance is given by the Ergun equation. The mass, momentum and energy balance equations of the mathematical model are given in Table 3. A detailed description of the mathematical model is presented elsewhere (Da Silva et al. 1999; Da Silva and Rodrigues 2001; Ribeiro et al. 2008).

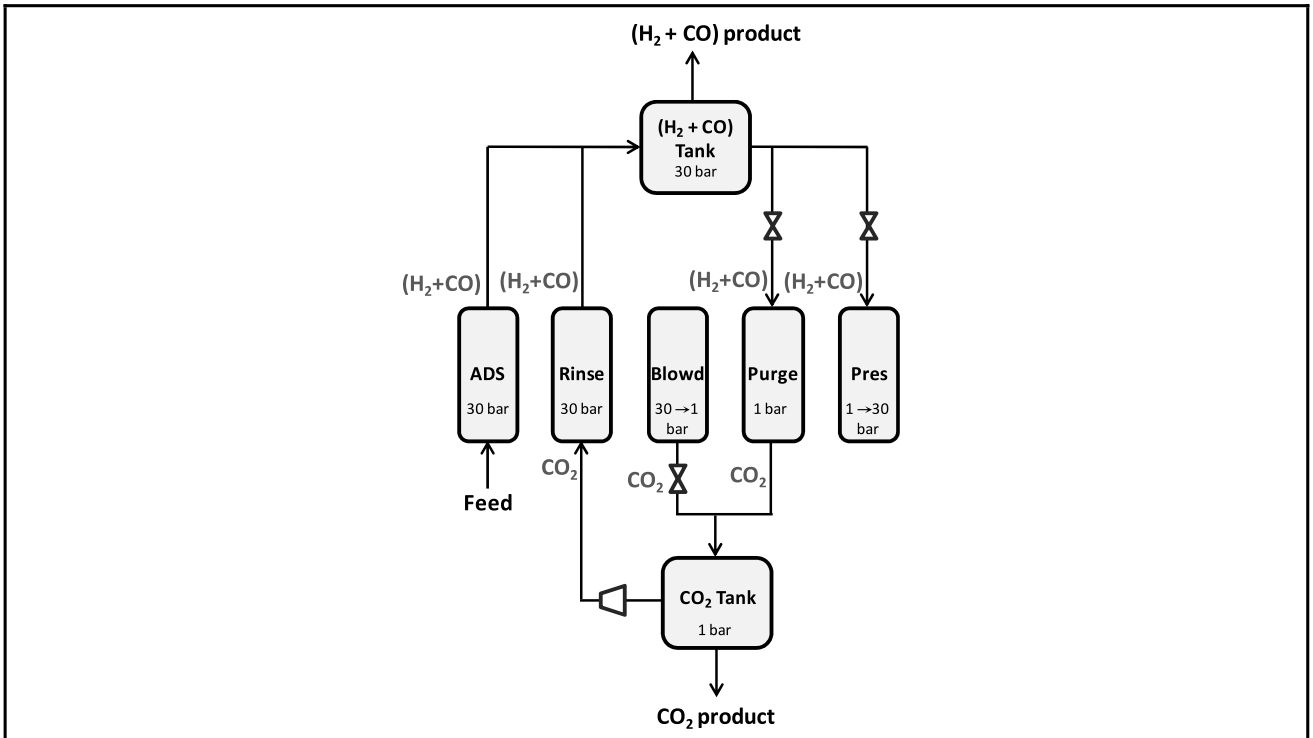

Adsorption		Rinse		Blowdown		Pg	Pressurization
Pg	Pressurization	Adsorption		Rinse		Blowdown	
Blowdown		Pg	Pressurization	Adsorption		Rinse	
Rinse		Blowdown		Pg	Pressurization	Adsorption	

Pg – purge

Fig. 2 PSA cycle and extended schedule to a 4-bed process

Table 3 Mass, momentum and energy balances of the mathematical model

Mass Balances

Gas Phase

$$\frac{\partial}{\partial z}(\varepsilon D_{\mathrm{ax}} C_{g,T}\frac{\partial y_i}{\partial z}) - \frac{\partial}{\partial z}(u_0 C_{g,i}) - \varepsilon\frac{\partial C_{g,i}}{\partial t} - \frac{(1-\varepsilon)a_p k_f}{1+Bi_i}(C_{g,i} - \overline{C_{p,i}}) = 0$$

Solid Phase—Macropore

$$\frac{\partial \overline{C_{p,i}}}{\partial t} = \frac{8D_{p,i}Bi_i}{R_p^2(1+Bi_i)}(C_{g,i} - \overline{C_{p,i}}) - \frac{\rho_p}{\varepsilon_p}\frac{\partial \overline{q_i}}{\partial t}$$

Solid Phase—Micropore

$$\frac{\partial \overline{q_i}}{\partial t} = \frac{3D_{c,i}}{r_c^2}(q_i^* - \overline{q_i})$$

Momentum Balance

$$-\frac{\partial P}{\partial z} = \frac{150\mu(1-\varepsilon)^2}{\varepsilon^3 d_p^2}u_0 + \frac{1.75(1-\varepsilon)\rho}{\varepsilon^3 d_p}|u_0|u_0$$

Energy Balances

Gas Phase

$$\frac{\partial}{\partial z}(\lambda\frac{\partial T_g}{\partial z}) - u_0 C_{g,T} C_p\frac{\partial T_g}{\partial z} + \varepsilon R_g T_g\frac{\partial C_{g,T}}{\partial t} - (1-\varepsilon)a_p h_f(T_g - T_p)$$
$$-\frac{4h_w}{d_{wi}}(T_g - T_w) - \varepsilon C_{g,T} C_V\frac{\partial T_g}{\partial t} = 0$$

Solid Phase

$$(1-\varepsilon)[\varepsilon_p\sum_{i=1}^{n}\overline{C_{p,i}}C_{v,i} + \rho_p\sum_{i=1}^{n}\overline{q_i}C_{v,\mathrm{ads},i} + \rho_p\hat{C}_{ps}]\frac{\partial T_p}{\partial t}$$
$$= (1-\varepsilon)\varepsilon_p R_g T_p\frac{\partial \overline{C_{p,T}}}{\partial t} + \rho_b\sum_{i=1}^{n}(-\Delta H_{\mathrm{ads}})_i\frac{\partial \overline{q_i}}{\partial t} + (1-\varepsilon)a_p h_f(T_g - T_p)$$

Column Wall

$$\rho_w\hat{C}_{p,w}\frac{\partial T_w}{\partial t} = \alpha_w h_w(T_g - T_w)$$

Table 4 Bed dimensions and adsorbent properties

Bed diameter (m)	3.5
Bed length (m)	8
Bed porosity	0.40
Adsorbent	Activated carbon Norit R2030
Adsorbent shape	Cylinders
Particle density (kg/m^3)	874
Pellet porosity	0.60
Pellet radius (m)	1.45×10^{-3}
Adsorbent surface area (m^2/g)	700
Particle specific heat (J/kg/K)	709

5 Results and discussion

The feasibility of the separation process presented in the previous sections was assessed by simulation.

The mathematical model was implemented in gProms environment (Process System Enterprise, London, UK) and solved using the orthogonal collocation on finite elements as the numerical method. The number of elements used was 60 with third order polynomials (two interior collocation points).

The dimensions of the beds were set to 8 m long and 3.5 m in diameter, which, with the specified feed flow rate, results in a superficial velocity of 0.04 m/s (or a molar flux per unit area of 47.6 mol/m^2/s). A bed porosity of 0.4 was assumed. A space time at feed conditions of 80 s is obtained. The adsorption capacity factor of carbon dioxide is 22.3 (calculated at feed conditions). The bed characteristics are summarized in Table 4 together with some properties of the adsorbent required for the simulation. In addition, the mathematical model employs several transport parameters. These were calculated using common correlations The axial mass (D_{ax}) and heat dispersion coefficients (λ), as well as, the mass transfer (k_f) and heat convective coefficients (h_f) were estimated using the Wakao and Funazkri correlations (Wakao and Funazkri 1978; Yang 1987; Da Silva 1999). The system was considered adiabatic. The convective heat transfer coefficient between the gas and the column wall (h_w) was calculated with the Wasch and Froment correlation (Wasch and Froment 1972). The macropore diffusivity (D_p) took into account only the molecular diffusivities which were calculated with the Chapman-Enskog equation (Bird et al. 2002). The micropore diffusivities (D_c) were determined experimentally by Grande et al. (2008). General properties of the gases, like density, viscosity, and molar specific heat were obtained according to Bird et al. (2002). The molar specific heat of the adsorbed gas was assumed to be equal to the molar specific heat in the gas phase (Sircar 1985). The transport parameters values used in the simulations are presented in Table 5.

Table 5 Transport parameters values used in the simulation

D_{ax} (m^2/s)	2.1×10^{-4}
λ (J/s/m/K)	2.6
k_f (m/s)	9.5×10^{-3}
h_f (W/m^2/K)	450
h_w (W/m^2/K)	285
D_p (m^2/s)[a]	CO_2: 5.10×10^{-7}
	H_2: 1.20×10^{-6}
	CH_4: 4.90×10^{-7}
	CO: 5.12×10^{-7}
	N_2: 4.67×10^{-7}
D_c/r_c^2 (s^{-1})[a]	CO_2: 4.44×10^{-2}
	H_2: 0.147
	CH_4: 1.57×10^{-2}
	CO: 1.45×10^{-1}
	N_2: 1.45×10^{-1}
μ (kg/m/s)[a]	1.6×10^{-5}
C_p (J/mol/K)[a]	31.3

[a]Values at inlet conditions

The feed flow rate and composition are presented in Table 1. The feed duration was set to 450 s and the purge duration to 100 s. A purge flow rate equal to the feed flow rate was employed. The rinse flow rate was optimized so that the required concentration of the carbon dioxide product could be obtained. This was achieved with a rinse flow rate of 0.266 m^3/s. Employing these operating parameters the results of Table 6 were obtained.

A light product that satisfies the feed requirement for the Fisher-Tropsch process was obtained. The H_2/CO stoichiometric ratio is 2.14 which is within the required range. The inerts content is also below the 15% limit recommended in the literature for allowing economic viability recycle of the biosyngas (Boerrigter et al. 2002).

A carbon dioxide product stream with purity of 95.18% was obtained with a considerable high recovery of CO_2—90.3%. The major impurity of the carbon dioxide is methane, that is, there are low amounts of hydrogen and carbon monoxide in the CO_2 product (the recovery of hydrogen is over 99% and the recovery of CO is over 98%).

The power consumption in the rinse compressor was also calculated. Adiabatic compression, multiple stages with the same pressure ratio and with a 5 psi pressure drop between stages was considered. It was also assumed that after each stage the gas is cooled back to the inlet temperature and an efficiency (η) of 85% was set. The equation used for the calculation is:

$$\text{Power} = \frac{1}{\eta}\dot{n}R_g T_1 \frac{\gamma}{\gamma - 1}\left(\left(\frac{P_2}{P_1}\right)^{\frac{\gamma-1}{\gamma}} - 1\right) \quad (5)$$

Table 6 Operating parameters and simulation results

Flow Rates (at operating conditions) (m^3/s)			
Feed		Rinse	Purge
0.388		0.226	0.388
Feed temperature (K)		P_{high} (bar)	P_{low} (bar)
303		30	1
Step times (s)			
Adsorption, Rinse, Blowdown		Pressurization	Purge
450		350	100
(Hydrogen + Carbon monoxide) product		Carbon dioxide product	Productivity (H_2 + CO) (mol/kg/day)
			166
Composition (%)	H_2/CO	Composition (%) Recovery (%)	Productivity (CO_2) (mol/kg/day)
CO_2: 3.73	2.14	CO_2: 95.18 90.3	62
H_2: 62.17		H_2: 0.36	
CH_4: 1.36	Inerts (%)	CH_4: 3.02	Power consumption in rinse compressor (MW)
CO: 29.11	8.72	CO: 1.32	3.36
N_2: 3.62		N_2: 0.12	

where $\dot{n}$ is the molar flow rate, R_g is the ideal gas constant, T_1 is the inlet temperature, P_1 and P_2 are respectively the inlet and outlet pressure and γ is the ratio between the heat capacity of the gas mixture at constant pressure and the heat capacity of the gas mixture at constant volume ($\gamma = \frac{C_p}{C_v}$) (McCabe et al. 1993; McAllister 2009). A value of 3.36 MW was obtained.

A Rectisol process requires more than 0.26 kWh/kg CO_2 at raw gas pressure of 25 bar for recovering 90% of CO_2 (Herzog 2000; Kunze and Spliethoff 2010). For the case studied 4.65 MW would be required by a Rectisol unit to capture the same amount of CO_2. This value is larger than the one required by the PSA unit.

The concentration and temperature profiles obtained at the end of each step at cyclic steady state are shown in Fig. 3. During adsorption the CO_2 concentration front moves forward in the bed. However, as the (H_2 + CO) product is produced during the adsorption and rinse steps, the adsorption step is stopped while the CO_2 front is still well within the bed. The rinse step that follows cleans the bed with CO_2 and desorbs the CO into the light product. The rinse step is carried until the CO_2 front reaches the end of the bed. At this point only a very small fraction of carbon monoxide and hydrogen remains in the bed. The carbon dioxide contained in the bed is then produced in the blowdown and purge steps. A fraction of the light product is then used to pressurize the bed. At the end of the pressurization step the bed is at the high adsorption pressure containing a very small amount of carbon dioxide.

The influence of the feed composition on the process performance was assessed with four simulations, where all the operation parameters were kept equal to the ones employed in the base case (Table 6) except the feed composition. In two of them, the (H_2 + CO) content was kept constant and the CO_2 content was changed 1% (respectively to 28.27 and 26.27%), balancing these changes with the minor impurities content. On the other two, the H_2 content was changed 1% (respectively to 46.45 and 44.45%), the H_2/CO ratio and the proportion of the remaining species was kept equal to the base case. The results obtained are shown in Table 7. It can be seen that the H_2/CO stoichiometric ratio is, in all cases, still within the specified range. However, when the CO_2 feed content decreases, the obtained CO_2 purity is below the 95% required (even thought its recovery does not change significantly).

The effect of the amount of light purge employed was also evaluated by changing the purge flow rate in two simulations, using respectively a purge flow rate equal to two times and half the feed flow rate. Once again all the remaining operating parameters were kept. The results obtained are presented in Table 8 where it can be observed that both the purity and recovery of CO_2 is affected. As the amount of purge used increases, the CO_2 purity decreases and the recovery increases.

As a change on the value of the feed pressure affects strongly the bed adsorption capacity, and the process performance changes significantly, an analysis of the effect of having a different feed pressure (for example caused by the use of a different pressure on the gasifier) was also made. A value of 25 bar was taken for study. If the same operating parameters are used with the new feed pressure value, a CO_2 product with a purity of 92.86% is obtained. The CO_2

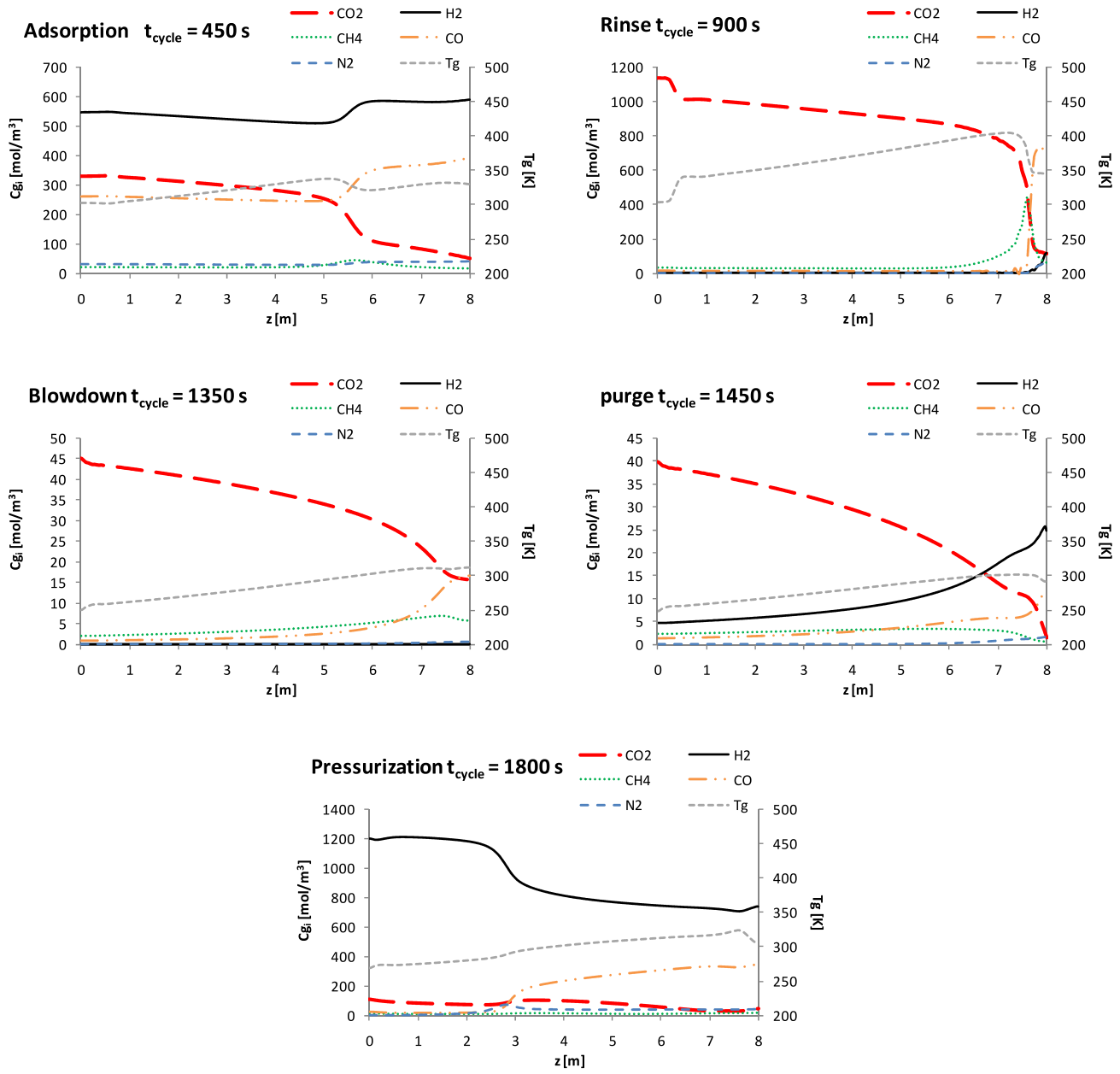

Fig. 3 Concentration and temperature profiles at the end of each step at cyclic steady state

Table 7 Effect of the feed composition on the process performance

Feed composition (%)					(H_2 + CO) product		CO_2 product	
CO_2	H_2	CH_4	CO	N_2	H_2/CO	Inerts (%)	Purity (%)	Recovery (%)
27.27	45.45	1.82	22.73	2.73	2.14	8.72	95.18	90.3
28.27	45.45	1.32	22.73	2.23	2.12	8.04	96.76	89.9
26.27	45.45	2.32	22.73	3.23	2.14	9.40	93.49	90.4
25.95	46.45	1.73	23.26	2.60	2.15	7.98	93.63	90.5
28.49	44.45	1.38	22.31	2.33	2.11	8.60	97.26	89.4

Table 8 Effect of the purge flow rate on the process performance

Purge flow rate (m^3/s)	($H_2 + CO$) product		CO_2 product	
	H_2/CO	Inerts (%)	Purity (%)	Recovery (%)
0.388	2.14	8.72	95.18	90.3
0.194	2.12	9.66	96.29	87.8
0.776	2.15	7.63	93.20	92.8

recovery also decreases to 84.9%. Adjusting the rinse flow rate in order to obtain a CO_2 purity of approximately 95.2%, the obtained recovery is even lower, 84.1%. That is, the CO_2 front breaks through the bed before the CO_2 content in the bed is high enough to produce a 95% CO_2 product. Consequently, the step times (or bed dimensions) should be adjusted to the new feed conditions. Using a feed duration of 400 s (keeping the constraints for the remaining steps imposed by 4-bed extension reported in the manuscript) and a rinse flow rate of 0.278 m^3/s, the following performance is obtained:

- ($H_2 + CO$) product: $H_2/CO = 2.13$; Inerts = 9.13%; Productivity = 166 mol/kg/day
- CO_2 product: Purity = 95.27%; Recovery = 89.2%; Productivity = 61 mol/kg/day
- Power consumption of the rinse compressor = 3.23 MW

These performance values are very close to the ones obtained in the 30 bar pressure case, which shows that with the appropriate adjustments of the operating parameters, the required separation performance can be obtained for different feed conditions.

These results show that the capture of CO_2 by PSA within a bio-syngas to Fisher-Tropsch process is a possible alternative to the commonly acid gas removal processes (Rectisol and Selesol).

6 Conclusions

The feasibility of replacing the absorbent-based processes (such as Rectisol and Selexol) for CO_2 capture by a pressure swing adsorption unit in a biomass to liquid system was evaluated.

A pressure swing adsorption cycle was developed to accomplish the required separation: production of a CO_2 stream ready for capture and production of a (H_2 + CO) stream with the required specifications of the Fischer-Tropsch reactor feed. The simulation results showed that a cycle with a feed duration of 450 s and a rinse flow rate of 0.266 m^3/s allows the production of CO_2 with a purity of 95.18% (proper for transport and sequestration) and a recovery of 90.3%. The H_2/CO stoichiometric ratio of the treated stream remained suitable for feeding the FT reactor (a H_2/CO ratio of 2.14 was obtained).

The power consumption of the CO_2 capture was found to be of 3.36 MW. This value represents a reduction of about 28% when compared to a Rectisol process with the same CO_2 recovery.

The influence of feed composition, amount of light purge and operating pressure on the process performance was assessed. It was found that the feed composition has a small impact in the process performance, except when the CO_2 feed content decreases more than 1%. For this case the CO_2 recovery decreases and the CO_2 purity constraint (purity > 95%) is not obeyed, although the stoichiometric ratio remains between the limits imposed.

The amount of light purge was found to influence both CO_2 purity and recovery. The CO_2 purity decreases and the recovery increases with the increase of the amount of purge.

It was found that if the operating pressure is decreased from 30 bar to 25 bar, at optimal operating conditions, the overall performance of the process remains the same, with a slight decrease of the power consumption.

The simulation results showed that a pressure swing adsorption process with a single adsorbent (activated carbon) is a valid alternative to the absorption-based processes currently used for CO_2 removal from bio-syngas.

Acknowledgement The authors thank LSRE financing by FEDER/POCI/2010.

References

Aasberg-Petersen, K., Christensen, T.S., Dybkjar, I., Sehested, J., Østberg, M., Coertzen, R.M., Keyser, M.J., Steynberg, A.P.: Synthesis gas production for FT synthesis. In: Steynberg, A., Dry, M. (eds.): Fischer-Tropsch Technology. Studies in Surface Science and Catalysis, vol. 152, pp. 258–405. Elsevier, Amsterdam/Boston (2004)

Batdorf, J.A.: Method and apparatus for methanol and other fuel production. U.S. Patent 7,655,703 (2010)

Bird, R.B., Stewart, W.E., Lightfoot, E.N.: Transport Phenomena, 2nd edn. Wiley, Singapore (2002)

Boerrigter, H., Uil, H.d., Calis, H.-P.: Green diesel from biomass via Fischer-Tropsch synthesis: new insights in gas cleaning and process design. Paper presented at the "Pyrolysis and Gasification of Biomass and Waste", Expert Meeting, Strasbourg, France, 30 September–1 October

Boerrigter, H.: Economy of biomass-to-liquids (BTL) plants: an engineering assessment. ECN Biomass, Coal & Environmental Research (2006). http://www.thermalnet.co.uk/docs/2G-1%20ECN-C-06-0191.pdf Accessed 30 July 2010

Chlendi, M., Tondeur, D.: Dynamic behavior of layered columns in pressure swing adsorption. Gas Sep. Purif. **9**(4), 231–242 (1995)

Da Silva, F.A.: Cyclic adsorption processes: application to propane/propylene separation. University of Porto (1999)

Da Silva, F.A., Silva, J.A., Rodrigues, A.E.: A general package for the simulation of cyclic adsorption processes. Adsorption **5**(3), 229–244 (1999)

Da Silva, F.A., Rodrigues, A.E.: Vacuum swing adsorption for propylene/propane separation with 4A zeolite. Ind. Eng. Chem. Res. **40**(24), 5758–5774 (2001)

Demirbas, A.: Biorefineries: current activities and future developments. Energy Convers. Manag. **50**(11), 2782–2801 (2009)

Drage, T.C., Blackman, J.M., Pevida, C., Snape, C.E.: Evaluation of activated carbon adsorbents for CO_2 capture in gasification. Energy Fuels **23**, 2790–2796 (2009)

Dry, M.: Chemical concepts used for engineering purposes. In: Steynberg, A., Dry, M. (eds.): Fischer-Tropsch Technology. Studies in Surface Science and Catalysis, vol. 152, pp. 196–257. Elsevier, Amsterdam/Boston (2004)

EPA: Alternative fuels: Fischer-Tropsch. Fact sheet number EPA420-F-00-036. http://www.afdc.energy.gov/afdc/pdfs/epa_fischer.pdf (2002). Accessed 30 July 2010

Fischer, F., Tropsch, H.: Die Erodölsynthese bei gewöhnlichem Druck aus den Vergangsprodukten der Kohlen. Brennst.-Chem. **7**, 97–104 (1926)

Fuderer, A., Rudelstorfer, E.: Selective adsorption process. U.S. Patent 3,986,849 (1976)

Grande, C.A., Lopes, F.V.S., Ribeiro, A.M., Loureiro, J.M., Rodrigues, A.E.: Adsorption of off-gases from steam methane reforming (H_2, CO_2, CH_4, CO and N_2) on activated carbon. Sep. Sci. Technol. **43**, 1338–1364 (2008)

Herzog, H.: The Economics of CO_2 Separation and Capture. http://sequestration.mit.edu/pdf/economics_in_technology.pdf (2000). Accessed 30 July 2010

Higman, C., van der Burgt, M.: Gasification, 2nd edn. Elsevier, Amsterdam (2008)

Kuester, J.L., Scottsdale, A.: Process of producing liquid hydrocarbon fuels from biomass. U.S. Patent 4,678,860 (1987)

Kumar, R., Kratz, W.C.: Separation of Multicomponent Gas Mixtures by Selective Adsorption. U.S. Patent 5,133,785 (1992)

Kunze, C., Spliethoff, H.: Modelling of an IGCC plant with carbon capture for 2020. Fuel Process. Technol. **91**(8), 934–941 (2010)

Lu, Y.J., Lee, T.: Influence of the feed gas composition on the Fischer-Tropsch synthesis in commercial operations. J. Nat. Gas Chem. **16**(4), 329–341 (2007)

Lv, P.M., Chang, J., Xiong, Z.H., Huang, H.T., Wu, C.Z., Chen, Y., Zhu, J.X.: Biomass air-steam gasification in a fluidized bed to produce hydrogen-rich gas. Energy Fuels **17**(3), 677–682 (2003)

McAllister, E.W.: Pipeline Rules of Thumb Handbook—Quick and Accurate Solutions to Your Everyday Pipeline Engineering Problems, 7th edn. Elsevier, Amsterdam (2009)

McCabe, W.L., Smith, J.C., Harriot, P.: Unit Operation of Chemical Engineering, 5th edn. McGraw-Hill, New Work (1993)

Ribeiro, A.M., Grande, C.A., Lopes, F.V.S., Loureiro, J.M., Rodrigues, A.E.: A parametric study of layered bed PSA for hydrogen purification. Chem. Eng. Sci. **63**, 5258–5273 (2008)

Sircar, S.: Excess properties and thermodynamics of multicomponent gas adsorption. J. Chem. Soc., Faraday Trans. **81**, 1527–1540 (1985)

Takeshita, T., Yamaji, K.: Important roles of Fischer-Tropsch synfuels in the global energy future. Energ Policy **36**(8), 2773–2784 (2008)

Taqvi, S.M., LeVan, M.D.: Virial description of two-component adsorption on homogeneous and heterogeneous surfaces. Ind. Eng. Chem. Res. **36**, 2197–2206 (1997)

Unruh, D., Pabst, K., Schaub, G.: Fischer-Tropsch synfuels from biomass: maximizing carbon efficiency and hydrocarbon yield. Energy Fuels **24**, 2634–2641 (2010)

Wakao, N., Funazkri, T.: Effect of fluid dispersion coefficients on particle-to-fluid mass transfer coefficients in packed beds. Chem. Eng. Sci. **33**(10), 1375–1384 (1978)

Wasch, A.P.D., Froment, G.F.: Heat transfer in packed beds. Chem. Eng. Sci. **27**, 567–576 (1972)

Yang, R.T.: Gas separation by adsorption processes. Butterworths, Boston (1987)

Yin, X.L., Leung, D.Y.C., Chang, J., Wang, J.F., Fu, Y., Wu, C.Z.: Characteristics of the synthesis of methanol using biomass-derived syngas. Energy Fuels **19**(1), 305–310 (2005)

Zhang, J., Webley, P.A.: Cycle development and design for CO_2 capture from flue gas by vacuum swing adsorption. Environ. Sci. Technol. **42**(2), 563–569 (2008)